Phys. Rev. Letters 28, 671 (1972).
[23]N. E. Christiensen, Solid State Commun. 9, 749 (1971).
[24]G. Grimvall, Physik Kondensierten Materie 11, 279 (1970).
[25]J. Moriarty, Phys. Rev. B 1, 1363 (1970).
[26]S. K. Sinha (private communication).

PHYSICAL REVIEW B VOLUME 6, NUMBER 10 15 NOVEMBER 1972

Electronic Phase Transitions of Cerium Metal*

Miguel Kiwi
Facultad de Ciencias, Universidad de Chile, Casilla 653, Santiago, Chile

and

Ricardo Ramírez
Instituto de Física, Universidad Católica de Chile, Casilla 114-D, Santiago, Chile
(Received 12 January 1972)

The model recently proposed by Ramírez and Falicov is generalized by the incorporation of the spin-orbit splitting of the $4f$ shell. This generalization provides an understanding of the fractional valence and magnetic susceptibility of α-cerium and suggests a mechanism to drive the α-α' phase transition.

I. INTRODUCTION

Phase transitions of Ce metal have received a great deal of attention in recent publications.[1-3] A p-T phase diagram (as given in Refs. 2 and 3) shows the following most relevant properties of the different forms Ce metal takes: The β and γ phases exhibit a magnetic moment close to the value of a singly occupied $4f$ shell. The α phase shows about one-fourth of the magnetic susceptibility of the γ phase,[1] while the α' phase has been found to be superconducting,[4] which implies that it has very weak magnetic properties. On the other hand, the β phase undergoes an antiferromagnetic transition at 12.5 °K making Ce the only known element to have both magnetic and superconducting phases.[1]

In this paper we also focus our attention on the α-α' phase transition for which the available experimental knowledge can be summarized as follows: (a) At room temperature the transition is observed[2] to occur at about 50 kbar; (b) the superconducting transition temperature[4] is 1.8 °K; (c) there is no agreement with regard to the crystal structure of the α' phase,[2] but the lattice parameter has been determined as 4.66 Å, while the α phase is known to be fcc with a lattice constant of 4.73 Å; and (d) the α phase has a valence of 3.67 ± 0.09, intermediate between the γ-phase value of about 3.0 and the α' phase which is assumed to be a truly four-valent metal.[1]

From the theoretical point of view, Ramírez and Falicov[3] (RF) recently proposed a model to explain the γ-α phase transformation of Ce. They assumed that the transition was driven by the promotion of one electron from an f orbital in the γ phase to the s-d conduction band in the α phase.[3] This implies that the α phase would consist of nonmagnetic Ce^{4+}-ion cores and four conduction electrons per atom, and therefore does not agree completely with the experimental results mentioned above.

In this paper we generalize the RF model in order to achieve a satisfactory agreement with experiment and suggest a mechanism to explain the α-α' phase transition. The main feature of our generalization is to incorporate the spin-orbit splitting of the $4f$ shell into the theory; this is achieved by introducing a doubly peaked density of f states in order to allow electrons to populate both the $J = \frac{5}{2}$ ground state or the $J = \frac{7}{2}$ excited state of the Ce atom.

In a certain way our model incorporates, and provides a formalism for, qualitative ideas outlined by Maple and Wohlleben[5] in relation to SmS, which in turn are based on a recent proposal of Hirst[6]; a discussion of this aspect is given in Sec. IV.

The general outline of this paper is as follows: After the present introduction a significantly improved solution of the RF model is given in Sec. II. On the basis of this solution, the generalized theory, which includes the spin-orbit splitting of the $4f$ shell, is developed in Sec. III. A full account of the minimization procedure of the pertinent forms of the Helmholtz free energy, its evaluation as well as the phase transitions and critical behavior that result, are given both in Secs. II and III. The paper is closed in Sec. IV with a critical discussion of the theory, in the

light of the available experimental information, which allows several conclusions to be drawn.

II. IMPROVED SOLUTION OF RF MODEL

A. Minimization of Helmholtz Free Energy

In this section we provide a significantly improved solution to the RF model; this solution is essential for the generalization which we propose below. The RF expression for the Helmholtz free energy F is

$$F = N\int_0^{W_e} D(\epsilon)[\epsilon n_e(\epsilon) + k_B T K_e(\epsilon)]\,d\epsilon + N\int_0^{W_h} D(\epsilon)[\epsilon n_h(\epsilon) + k_B T K_h(\epsilon)]\,d\epsilon + N[Ef + k_B T(K_f - f\ln q) - Gf^2], \quad (2.1)$$

where $D(\epsilon) = 12/(W_e + W_h)$ is the constant s-d-like density of states per atom and unit energy, W_e and W_h are the maximum electron and hole excitation energies, respectively, measured, as all energies throughout this paper, relative to the Fermi level. G is the repulsive (attractive) interaction between f-shell and s-d-band electrons (holes). In this paper, as in RF, we take $W_e = 5.44$ eV and $W_h = 2.72$ eV. n_e, n_h, and f are the occupation probabilities of conduction electrons, holes, and f-like electrons, respectively,

$$K = n\ln n + (1-n)\ln(1-n),$$

k_B is the Boltzmann factor, and $q = 2J+1$ is the ionic multiplicity of the Ce atoms.

Conservation of charge requires that

$$\int_0^{W_h} D(\epsilon)\, n_h(\epsilon)\,d\epsilon - \int_0^{W_e} D(\epsilon)\, n_e(\epsilon)\,d\epsilon = f. \quad (2.2)$$

The Helmholtz free energy F is now minimized, with respect to n_e, n_h, and f, under the constraint imposed by Eq. (2.2) taken into account through the use of Lagrange multipliers. The following results are then obtained:

$$n_e(\epsilon) = \left[a^{-1}\exp\left(\frac{\epsilon - E + 2Gf}{k_B T}\right) + 1\right]^{-1}, \quad (2.3)$$

$$n_h(\epsilon) = \left[a\exp\left(\frac{\epsilon + E - 2Gf}{k_B T}\right) + 1\right]^{-1}, \quad (2.4)$$

and

$$f = \frac{12 k_B T}{W_e + W_h}\ln\left|\frac{A_e + e^{-Q_e}}{A_h + e^{-Q_h}}\,\frac{A_h + 1}{A_e + 1}\right|, \quad (2.5)$$

where

$$a \equiv f/[(2J+1)(1-f)], \quad (2.6)$$

$$A_h = \frac{1}{A_e} \equiv a\exp\left(\frac{E - 2Gf}{k_B T}\right), \quad (2.7)$$

$$Q_h \equiv W_h/k_B T, \quad (2.8)$$

$$Q_e \equiv W_e/k_B T. \quad (2.9)$$

Equation (2.5) is the basic result of the minimization procedure; it is an implicit equation for the equilibrium value of f as a function of temperature, and depends also on the parameters of the system (i.e., W_e, W_h, E, G, and J). For a given set of parameters and a fixed value of T, Eq. (2.5) may yield one or three solutions; in the latter case one corresponds to a maximum of F and the other two to local minima.

B. Evaluation of Free Energy

For the values of W_e and W_h assumed above, we can see that Q_e and Q_h are quite large; we therefore try the following expansion of the right-hand side of Eq. (2.5):

$$f = \frac{12 k_B T}{W}\ln A_e + \frac{12 k_B T}{W}\left(\frac{e^{-Q_e}}{A_e} - \frac{e^{-Q_h}}{A_h}\right), \quad (2.10)$$

where we have defined W as

$$W \equiv W_e + W_h. \quad (2.11)$$

Neglecting the terms containing exponentials in (2.1), we obtain

$$A_e = e^{Wf/12 k_B T}, \quad (2.12)$$

and within this approximation

$$\frac{e^{-Q_e}}{A_e} = \exp\left[-\left(2 + \frac{f}{4}\right)\frac{W}{3 k_B T}\right], \quad (2.13)$$

$$\frac{e^{-Q_h}}{A_h} = \exp\left[-\left(1 - \frac{f}{4}\right)\frac{W}{3 k_B T}\right]. \quad (2.14)$$

Since we are concerned only with temperatures lower than 1000 °K, the ratio $W/3k_B T > 30$; therefore, we are fully justified in neglecting the exponential terms in Eq. (2.10) and we can safely use the expression (2.12) for A_e from now on. This yields

$$\tfrac{1}{12} W f = -E + 2Gf - k_B T\ln[f/q(1-f)], \quad (2.15)$$

which can be used advantageously to calculate the free energy.

For convenience, we write

$$F = F_1 + F_2 + F_3, \quad (2.16)$$

where F_1, F_2, and F_3 are the first, second, and third terms on the right-hand side of (2.1), respectively. After the definition of $x \equiv \epsilon/k_B T$, it is easy to see that the limits of integration can be replaced by infinity in (2.1), and since we can write

$$K_s = -x n_s - n_s\ln A_s + \ln(1 - n_s), \quad (2.17)$$

where s denotes either electron or hole (e or h), we obtain the following results (see the Appendix):

$$\int_0^{\infty} \ln[1 - n_s(x)]\,dx$$

$$= -\frac{\pi^2}{6} - \frac{\mu_s^2}{2} - \sum_{\nu=1}^{\infty} \frac{(-1)^\nu}{\nu^2} e^{\nu\mu_s}, \quad \mu_s \leq 0$$

$$= \sum_{\nu=1}^{\infty} \frac{(-1)^\nu}{\nu^2} e^{-\nu\mu_s}, \quad \mu_s \geq 0 \qquad (2.18)$$

where $\mu_s \equiv \ln A_s$ and

$$\int_0^\infty n_s(x)\,dx = \ln(1 + 1/A_s) . \qquad (2.19)$$

The explicit evaluation of these integrals allows us to write the following expressions for F_1 and F_2:

$$F_1 = \frac{12(k_B T)^2}{W} N\Big(\sum_{\nu=1}^{\infty} \frac{(-1)^\nu}{\nu^2} \frac{1}{A_e^\nu} - \ln A_e \ln(A_e + 1) + (\ln A_e)^2 \Big) \qquad (2.20)$$

and

$$F_2 = \frac{12(k_B T)^2}{W} N\Big(-\tfrac{1}{2}(\ln A_e)^2 - \tfrac{1}{6}\pi^2 - \sum_{\nu=1}^{\infty} \frac{(-1)^\nu}{\nu^2} \frac{1}{A_e^\nu} + \ln A_e \ln(A_e + 1) \Big) . \qquad (2.21)$$

Combination of (2.1), (2.16), (2.20), and (2.21) yields a remarkably simple final form for the total Helmholtz free energy F, which reads

$$\frac{F}{N} = -\frac{2\pi^2(k_B T)^2}{W} + \frac{W f^2}{24} + Ef - Gf^2 + k_B T(K_f - f \ln q) . \qquad (2.22)$$

From this expression we can obtain all the thermodynamic information about our system.

C. α-γ Phase Transition

As mentioned above, Eq. (2.5) may yield one or three solutions for f, for a given set of parameters and a fixed value of T. Let us consider the latter case and call f_1 and f_2 the solutions corresponding to local minima of F at the transition temperature T_0.

Equation (2.15) then implies that

$$\rho f_1 - E - k_B T_0 \ln \frac{f_1}{q(1 - f_1)} = 0 , \qquad (2.23)$$

$$\rho f_2 - E - k_B T_0 \ln \frac{f_2}{q(1 - f_2)} = 0 , \qquad (2.24)$$

where the definition $\rho \equiv 2G - \frac{1}{12} W$ has been used.

A phase transition does occur when both phases have equal free energy, that is, when

$$F(f_1, T_0, N) = F(f_2, T_0, N) , \qquad (2.25)$$

which, from (2.15) and (2.22), can be written as

$$\tfrac{1}{2}\rho(f_1^2 - f_2^2) - E(f_1 - f_2) - k_B T_0 \Big(f_1 \ln \frac{f_1}{q(1 - f_1)} - f_2 \ln \frac{f_2}{q(1 - f_2)} - \ln \frac{1 - f_1}{1 - f_2} \Big) = 0 . \qquad (2.26)$$

The parameter E and the transition temperature T_0 can be eliminated from (2.23), (2.24), and (2.26), to obtain the relation

$$(f_1 + f_2) \ln \frac{f_1}{f_2} = (2 - f_1 - f_2) \ln \frac{1 - f_2}{1 - f_1} . \qquad (2.27)$$

This equation provides, apart from the trivial solution $f_1 = f_2$, the most important result

$$f_1 + f_2 = 1 , \qquad (2.28)$$

which constitutes a sum rule that the values of f must satisfy at the transition point.

Addition of (2.23) and (2.24) and use of the above sum rule allows us to obtain immediately a linear relation between E and T_0. It should be mentioned that this linear relation was obtained as a best-fit curve in the RF paper, while we obtain it here as a rigorously derived consequence of the model. The analytic form of the relation is

$$E = \tfrac{1}{2}\rho + (k_B \ln q)\, T_0 . \qquad (2.29)$$

It is apparent that the same result is obtained when $f = \frac{1}{2}$ is replaced in Eq. (2.15), which clearly indicates that $f = \frac{1}{2}$ is the third solution of (2.5) corresponding therefore to the branch with *maximal* free energy.

Finally, using the experimentally determined relation between the transition temperature T_0 and the applied pressure p,

$$T_0 = T_A + cp , \qquad (2.30)$$

where $T_A = 116\,^\circ\mathrm{K}$ and $c = 23.73\,^\circ\mathrm{K/kbar}$, we obtain

$$E = E_0 + Bp , \qquad (2.31)$$

where $E_0 \equiv \frac{1}{2}\rho + k_B T_A \ln q$ and $B \equiv k_B c \ln q$. This relation is consistent with the basic assumption that the localized $4f$ shells move away from the Fermi surface with increasing pressure.

D. Critical Point

A critical point, which the RF model yields, is the point at which a sharp phase transition ceases to occur and a smooth transition begins to take place; an illustration of this case is given in Fig. 4 of the RF paper. Analytically, the critical point is determined by requiring that both of the two following conditions be satisfied:

$$\frac{\partial(1/T)}{\partial f} = 0 \qquad (2.32a)$$

and

$$\frac{\partial^2(1/T)}{\partial f^2} = 0 . \qquad (2.32b)$$

Use of Eq. (2.5) immediately gives

$$\frac{\rho - k_B T/f(1 - f)}{k_B \ln[f/q(1 - f)]} = 0 \qquad (2.33a)$$

and

$$\frac{(1-2f)}{k_B f^2(1-f)^2 \ln[f/q(1-f)]} = 0 , \qquad (2.33b)$$

and since at the critical point the three solutions for f merge into one we have $f=\frac{1}{2}$ at the critical temperature T_c, which is therefore given by

$$k_B T_c = \tfrac{1}{4}\rho . \qquad (2.34)$$

We return now, for a moment, to Eq. (2.15) to point out that it can also be written as

$$f=\{\exp[(E-\mu)/k_B T]+1\}^{-1} , \qquad (2.35)$$

where we used the definition $\mu \equiv \rho f + k_B T \ln q$. We observe that phase transitions do occur at temperatures for which the argument of the exponential vanishes; this again gives the result $f = f_{\text{critical}} = \frac{1}{2}$ which shows the internal consistency of this scheme.

Equation (2.35) is of great importance for our purposes and we will return to discuss its implications in Sec. III. For the time being let us simply mention that the α-γ phase transition occurs when the condition $E=\mu$ is satisfied; when $E<\mu$ we are in the γ phase, with populated $4f$ levels; while for $E>\mu$ the α phase is stable and the f levels become depopulated. As a consequence, a valence increase of one unit and a large change in magnetic susceptibility should be observed experimentally, which is not the case; on this shortcoming of the theory we focus our attention in Sec. III.

III. SPIN-ORBIT SPLITTING OF 4f SHELL

A. Minimization of Helmholtz Free Energy

In this section we generalize the RF model by incorporating the spin-orbit splitting of the $4f$ shell into the theory; the $4f$ electrons are now shared between two localized f-like states. The ground state has $J=\frac{5}{2}$ while the excited state corresponds to $J=\frac{7}{2}$ and the energy difference ξ between them is estimated to be $\xi \sim 0.3$ eV.

We characterize this ionic structure by the density of states

$$\rho(\epsilon) = \tfrac{6}{14}\delta(\epsilon - E') + \tfrac{8}{14}\delta(\epsilon - E) , \qquad (3.1)$$

such that $\xi = E - E' > 0$, where E is the energy of the excited $J=\frac{7}{2}$ state and E' the energy of the $J=\frac{5}{2}$ ground state. The values of $\frac{6}{14}$ and $\frac{8}{14}$ are due to the different degeneracy of the ground and excited states, respectively. This allows us to write the Helmholtz free energy F of the system, including spin-orbit effects, as

$$F = N\int_0^{W_e} D(\epsilon)[\epsilon n_e(\epsilon) + k_B T K_e(\epsilon)]\,d\epsilon$$

$$+N\int_0^{W_h} D(\epsilon)[\epsilon n_h(\epsilon) + k_B T K_h(\epsilon)]\,d\epsilon$$

$$+N\int_{-\infty}^{\infty} \rho(\epsilon)[\epsilon n_f(\epsilon) + k_B T K_f(\epsilon)]\,d\epsilon$$

$$-NG[\tfrac{6}{14} n_f(E') + \tfrac{8}{14} n_f(E)]^2$$

$$-Nk_B T[\tfrac{6}{14} n_f(E')\ln q' + \tfrac{8}{14} n_f(E)\ln q] , \qquad (3.2)$$

where most of the notation was defined after Eq. (2.1). The only new symbols are the occupation probability for f-like electrons, n_f, and the ionic multiplicities of the $J=\frac{7}{2}$ and $J=\frac{5}{2}$ states, denoted by q and q', respectively.

The equation of conservation of charge now requires that

$$\int_0^{W_h} D(\epsilon) n_h(\epsilon)\,d\epsilon - \int_0^{W_e} D(\epsilon) n_e(\epsilon)\,d\epsilon = \int_{-\infty}^{\infty} \rho(\epsilon) n_f(\epsilon)\,d\epsilon . \qquad (3.3)$$

The right-hand side of the above relation represents the average occupation of the $4f$ levels which we denote by f, as we did for the equivalent quantity in Sec. II. The free energy can now be minimized under the constraint (3.3), following the scheme given in Sec. II, to obtain an expression for f; it reads

$$f = \frac{6}{14}\left[\exp\left(\frac{E'-\mu'}{k_B T}\right)+1\right]^{-1} + \frac{8}{14}\left[\exp\left(\frac{E-\mu}{k_B T}\right)+1\right]^{-1} , \qquad (3.4)$$

where, as before, $\mu \equiv f + k_B T \ln q$ and similarly $\mu' \equiv f + k_B T \ln q'$.

B. Phase Transitions

Equation (3.4) is the generalization of (2.35) and it allows a direct discussion of the physical consequences of our model. In order to carry out this discussion we make the physically reasonable, and otherwise simplifying assumption, that the pressure dependence of *both* the $J=\frac{5}{2}$ and the $J=\frac{7}{2}$ $4f$ levels is given by relations of the form (2.31), as derived in Sec. II. That is, E and E' are assumed to be linearly dependent on pressure with the same slope (given by the coefficient B), but with different values of the intercept.

With this assumption in mind we consider the process of applying pressure at constant temperature. At sufficiently low pressures, $E' \ll \mu'$ and $E<\mu$; as the applied pressure is increased, E grows until it equals and eventually becomes larger than μ. On this basis Eq. (3.4) allows a quite accurate semiquantitative analysis of the values that f takes; at first both Fermi functions are nearly equal to unity and therefore f takes values only slightly smaller than 1. When $E=\mu$ the second term on the right-hand side decreases, quite abruptly, from nearly $\frac{8}{14}$ to approximately 0 and f drops from a value slightly less than 1 to around

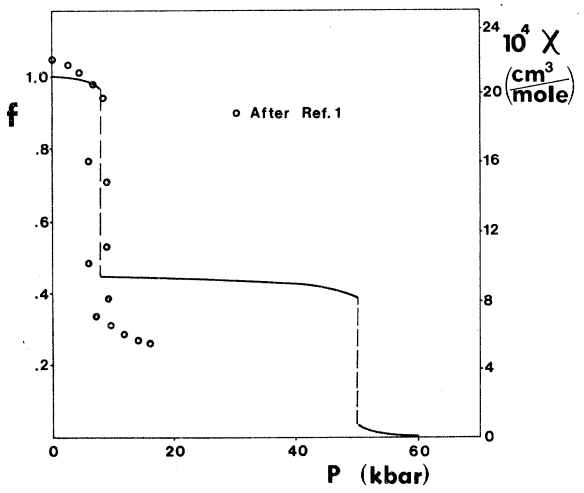

FIG. 1. Plot of the calculated values of f, the average occupation of $4f$ levels, and the magnetic susceptibility χ vs pressure p.

$\frac{6}{14}$: We identify this change as the $\gamma \rightarrow \alpha$ transition, now with a fractional valence change, since the valence simply is given by $4-f$.

As the pressure is increased further, beyond the $\gamma \rightarrow \alpha$ transition, the condition $E' = \mu'$ is eventually satisfied and a second transition does take place: the $\alpha \rightarrow \alpha'$ transition. As expected, f drops from the value near $\frac{6}{14}$ to approximately zero. The analysis outlined above is in over-all agreement with the quantitative results obtained through numerical computation; a plot of f vs pressure, for a temperature of 296 °K, is given in Fig. 1. The parameters E and E' were used to fit the experimental values of the transition pressures, at the above given temperature of 296 °K; their difference turns out to be $\xi = E - E' = 0.33$ eV, in excellent agreement with the magnitude of the spin-orbit splitting of the $4f$ shell, estimated to be $\xi \sim 0.3$ eV.

The precise resultant values for the valence of the γ, α, and α' phases turn out to be 3.02, 3.56, and 3.97, respectively, in very reasonable agreement with experimental results[2] which in the particular case of α-Ce yield 3.67 ± 0.09.

The main contribution to the magnetic susceptibility of cerium is due to the well-localized $4f$ electrons. Therefore, we may assume that χ obeys Curie's law,[7] i.e., it is linearly proportional to the average occupation f as defined after (3.3), according to the expression[7]

$$\chi = \frac{N g J(J+1)\mu_B^2}{3k_B} \frac{f}{T} , \tag{3.5}$$

where μ_B is the Bohr magneton and $g = 0.811$ is the pertinent value[7] for Ce. A plot of χ vs p is also given in Fig. 1, with the magnitude of the susceptibility indicated on the right-hand-side ordinate; the experimental values reported in Ref. 1 are also plotted, for comparison purposes. It is noticed that the susceptibility drop of the $\gamma \rightarrow \alpha$ transition predicted by our theory is in good agreement with experiment. The pressure dependence of χ is less consistent with the observed results, which we attribute to the unrealistic forms we have used for the densities of states: constant for the s-d conduction band and δ-function-like for the $4f$ shells. The predicted value of χ for the α' phase seems quite reasonable; in fact, it is practically the same as the extrapolated value given in Ref. 1, and thus almost identical to the magnetic susceptibility of Hf and Th which, as the α' phase of Ce, are superconductors.

Finally, it should be mentioned that the calculated values of χ contain no adjustable parameter, which makes the good agreement reached with the presently available experimental information very satisfactory.

C. Critical Behavior and Transition Lines

We first consider the γ-α phase change; near this transition Eq. (3.4) can be written as

$$f \cong \frac{6}{14} + \frac{8}{14}\left[\exp\left(\frac{E-\mu}{k_B T}\right) + 1\right]^{-1} . \tag{3.6}$$

As indicated before, a critical point is determined by the conditions (2.32a) and (2.32b). They give, in this case, the following critical value for f:

$$f_c = \tfrac{6}{14} + \tfrac{1}{2} \cdot \tfrac{8}{14} = \tfrac{5}{7} , \tag{3.7}$$

and the critical temperature turns out to be

$$k_B T_c = \tfrac{1}{7}\rho . \tag{3.8}$$

It is now easy to realize, recalling the argument given after (2.35) in Sec. II, that the γ-α transition temperature T_0 satisfies the linear relation

$$E = \tfrac{5}{7}\rho + (k_B \ln q)\, T_0 . \tag{3.9}$$

It is quite clear that this treatment follows very closely the one given before (i.e., in Sec. II), because it is possible to approximate Eq. (3.4) by (3.6), with great accuracy, near the γ-α transition. Of course, a similar procedure can be applied to the α-α' transition, near which we can write

$$f \cong \frac{6}{14}\left[\exp\left(\frac{E'-\mu'}{k_B T}\right) + 1\right]^{-1} , \tag{3.10}$$

which quite straightforwardly would yield a critical point and its characteristics; however, this has not been observed experimentally so that we will not insist on this matter. The only important comment we add here is that the slope of the α-α' transition line turns out to be, in the context of

our model and in analogy to (3.9), $k_B \ln q'$ which is a positive quantity; experimental results[2] indicate, however, that the slope is negative, which we think constitutes the main shortcoming of our theory.

Our preliminary impression on this subject is that it could be related to the fact that the α-α' transition is not as sharp as the γ-α one, but instead it is a smooth transition accompanied by an *increase* in resistance,[8] which could be an indication that both an electronic and some kind of structural change occur simultaneously. However, in order to clarify this point more experimental information is necessary, mainly the determination of the crystal structure and the magnetic susceptibility of the α' phase.

IV. DISCUSSION AND CONCLUSIONS

We have generalized the model of RF, by incorporating the spin-orbit splitting of the $4f$ shell, in such a way as to account for the fractional valence and enhanced magnetic susceptibility of α-cerium. In previous work[3] the $\gamma \rightarrow \alpha$ transition had been explained on the basis of the promotion of a $4f$ electron to the s-d conduction band, which implies an integral valence change, from 3 to 4, and a very drastic reduction in magnetic susceptibility, which are in contradiction with experimental results.[1,2]

Together with removing these shortcomings of previous work we suggest a mechanism which could drive the α-α' phase transition; this mechanism is not inconsistent with a well-known property of α'-Ce: its superconductivity.

The basic physical picture which underlies our model is that the $J=\frac{7}{2}$ excited state, populated because of thermal excitation, and the $J=\frac{5}{2}$ ground state of the cerium $4f$ shells are "dumped" successively into the s-d conduction band, as pressure is increased, in two essentially discrete steps. The first step is related to the $\gamma \rightarrow \alpha$ transition and the second to the α-α' one. This physical picture is certainly borne out by the analytical procedure; the solution scheme consists of a significantly improved treatment of the RF model, given in Sec. II, which serves as a framework to the generalized theory, with spin-orbit coupling included, which is tackled in Sec. III.

The analytic treatment yields, as basic results, the expression for the average occupation of $4f$ levels, given by (3.4) and the plot of f and the magnetic susceptibility χ vs pressure, shown in Fig. 1. The agreement with the experimental measurements of χ, indicated as open circles in Fig. 1, is quite apparent; on the other hand, the calculated value for the valence of α-Ce turns out to be 3.56, while the measured result is 3.67 ± 0.09.

Some features of our theory, i.e., the fractional occupation of near-lying energy levels, seem to be closely related to a proposal put forward recently by Hirst[6] in relation to the Anderson model, although the formal context is quite different in both cases. The basic ideas of the proposal of Hirst were invoked recently by Maple and Wohlleben[5,9] to explain some features of the phase transitions of SmS and TmTe. It is our impression that our theory may be useful in achieving a formal and more detailed understanding of these transitions.

It has been suggested that hybridization between the $4f$ states and the s-d conduction band may play an important role in the description of the physical properties of Ce. We have treated this hybridization in several different ways, which demands significant analytic and numerical efforts, with no success. The results obtained in this way yield either no improvement or even worse agreement with experiment, when compared to the RF model.

In conclusion, we have generalized the RF model accounting for the experimentally observed values of the valence and magnetic susceptibility of the α phase of cerium. At the same time, we have provided a significantly improved solution of the model and suggested a mechanism to drive the α-α' phase transition. In our opinion, the main shortcoming of our work is that it yields the wrong sign for the slope of α-α' transition line on the p vs T plane.

ACKNOWLEDGMENTS

We gratefully acknowledge stimulating conversations with Dr. A. Sweedler and Dr. D. Wohlleben, and thank Dr. B. Chornik for the use of his computer.

APPENDIX

From Eqs. (2.3), (2.4), and (2.6), we obtain

$$\int_0^\infty \ln[1-n_s(x)]\,dx = \int_0^\infty \ln\left(\frac{e^{(x+\mu_s)}}{e^{(x+\mu_s)}+1}\right) dx \ ,$$

where $x=\epsilon/k_BT$ and $\mu_s=\ln A_s$. By changing the variable x to $z=e^{x+\mu_s}$, this is reduced to

$$-\tfrac{1}{2}\mu_s^2 - \int_{e^{\mu_s}}^\infty z^{-1}\ln(1+z)\,dz \ ,$$

where we have used $\int z^{-1}\ln z\,dz = \frac{1}{2}(\ln z)^2$. The integral in this last step can be found in tables[10]; then, by using the relation

$$\sum_{n=1}^{\infty} (-1)^{n+1} n^{-2} = \tfrac{1}{12}\pi^2 \ ,$$

we get the result (2.18).

*Work supported in part by CONICYT (Chilean National Commission for Research and Technology) and the University of Chile–University of California Cooperative Program (supported by the Ford Foundation).

[1]M. R. Mac Pherson, G. E. Everett, D. Wohlleben, and B. M. Maple, Phys. Rev. Letters 26, 20 (1971), and references cited therein.

[2]A. Jayaraman, Phys. Rev. 137, A179 (1965); E. Franceschi and G. L. Olcese, Phys. Rev. Letters 22, 1299 (1969); E. King, J. A. Lee, I. R. Harris, and T. F. Smith, Phys. Rev. B 1, 1380 (1970); D. B. Mac Whan, *ibid.* 1, 2826 (1970).

[3]R. Ramírez and L. M. Falicov, Phys. Rev. B 3, 2425 (1970).

[4]J. Wittig, Phys. Rev. Letters 21, 1250 (1968).

[5]M. B. Maple and D. Wohlleben, Phys. Rev. Letters 27, 511 (1971).

[6]L. Hirst, Physik Kondensierten Materie 11, 255 (1970).

[7]C. Kittel, *Introduction to Solid State Physics* (Wiley, New York, 1966), p. 437.

[8]E. King, European High Pressure Group Ninth Annual Meeting, Umea, Sweden, June, 1971 (unpublished).

[9]D. Wohlleben, J. G. Huber, and M. B. Maple (unpublished).

[10]See, for example, H. B. Dwight, *Tables of Integrals and Other Mathematical Data*, 4th ed. (Macmillan, New York, 1961), formula 621.1.

PHYSICAL REVIEW B VOLUME 6, NUMBER 10 15 NOVEMBER 1972

Azbel'–Kaner Cyclotron Resonance and Magnetic Surface Levels in Beryllium*

T. A. Kennedy† and G. Seidel
Brown University, Providence, Rhode Island 02912

(Received 19 June 1972)

Azbel'–Kaner cyclotron resonance in beryllium has been used to investigate the angular dependence of effective masses in the $(10\bar{1}0)$ and (0001) planes. The samples studied had a residual resistivity ratio of ~ 2000, producing at helium temperatures and 35-GHz values of $\omega\tau$ of approximately 10. Resonances were observed from belly and neck holes on the second-zone coronet and from electrons on the third-zone cigars. Where possible, results have been compared with effective masses obtained in de Haas–van Alphen experiments. Surface-impedance oscillations due to magnetic surface levels were also observed at low magnetic fields and 35 GHz. Oscillations due to electrons of two different sections of the Fermi surface can be distinguished in angular studies in the $(10\bar{1}0)$ plane. One set of oscillations, centered about the $\langle 11\bar{2}0\rangle$, has been ascribed to holes on the coronet necks. A second set, observed about the $\langle 0001\rangle$, is due either to holes on the ridge of the coronet belly or electrons on the ridge of the cigar waist. A comparison of the Fermi-surface parameters obtained in the surface-level experiments is made with known values for beryllium.

I. INTRODUCTION

A description of the electronic properties of a metal requires knowledge of the shape of the Fermi surface, derivatives of the energy at the Fermi surface, and the orbital-scattering times. Several experimental and theoretical studies of the topology of the beryllium Fermi surface have been carried out and are generally in good agreement. Recent de Haas–van Alphen (dHvA) studies include those of Watts[1] and Tripp *et al.*[2] An orthogonalized-plane-wave (OPW) calculation was performed by Loucks and Cutler[3] and Loucks[4] and a nonlocal-pseudopotential calculation by Tripp *et al.*[2] These studies have established that the beryllium Fermi surface consists of a second-zone hole surface (coronet) and third-zone electron surfaces (cigars) (see Fig. 1). The coronet has six large pieces, the bellies, joined by six almost cylindrical necks. The cigars have a cross section that is triangular near the center, changing continuously to circular near the hemispherical caps. The cigar waist is constricted giving minimum cross-sectional area in the ΓKM plane and maximum cross-sectional areas about one quarter the distance from K to H.

While the Fermi surface of Be has been extensively investigated using the dHvA effect, only a very few measurements[5,6] have been performed on this metal using Azbel'–Kaner cyclotron resonance (AKCR). As has been repeatedly demonstrated on many different metals,[7] AKCR can give detailed information of the effective masses of electrons on a variety of orbits in the Fermi surface.

In the Azbel'–Kaner geometry with the direction of the dc magnetic field in the plane of the surface of the metal slab, cyclotron resonance occurs by virtue of the electrons repeatedly arriving within the skin depth in phase with the rf field. Electrons with orbits having extremal mass values can produce a magnetic field dependence to the surface impedance provided their orbital lifetimes are sufficiently long. In this study of Be, effective masses have been obtained from a 35-GHz AKCR angular study of the $(10\bar{1}0)$ and (0001) planes. Resonances were observed and effective masses measured for carriers of the third-zone cigars and the bellies